Catalysis Letters Vol. 97, Nos. 1–2, August 2004 (© 2004)

# $n$-Hexane Isomerization over $NiO/SO_4^{2-}/ZrO_2$ catalysts. Effect of nickel loading

M. Perez-Luna, J.A. Toledo Antonio, A. Montoya, and R. Rosas-Salas

*Instituto Mexicano del Petróleo, Prog. de Ingeniería Molecular, Eje Central Lázaro Cárdenas No. 152, 07730 México, D.F. México*

Received 5 March 2004; accepted 27 May 2004

The effect of nickel addition to the sulfated $ZrO_2$ catalysts for $n$-hexane isomerization was investigated. A series of catalysts with different nickel concentration (from 0 to 9.6 wt%) were synthesized by supporting nickel on sulfated zirconia by incipient wetness method. After a calcination procedure the catalysts were characterized by X-ray diffraction, nitrogen physisorption (BET method) and its acidic properties were determined by $NH_3$ adsorption (TPD) and FT-IR of pyridine adsorption. The $n$-hexane isomerization reaction was carried out in a fixed bed microreactor at 673 K under 345 kPa of total pressure. Results showed that nickel content between 1.5 and 4.5 wt% improved the catalytic activity and favored the formation 2,3-dimethylbutane, which is a highly desired product. X-ray diffraction results showed no evidence of any NiO phase at NiO concentration below 9.6 wt% suggesting a NiO phase highly dispersed on the surface of $ZrO_2$–$SO_4^{2-}$ with crystallite sizes lesser than 3 nm. Catalytic activity and 2,3-dimethylbutane selectivity seems to be correlated with the NiO well dispersed phase rather than with their acidic properties.

**KEY WORDS:** sulfated zirconia; nickel promoted sulfated zirconia; $n$-hexane isomerization; acid catalysis.

## 1. Introduction

The increasing interest in improving the environmental protection and to promote the efficiency of the automotive motors encourages the formulation of new catalysts and the development of new processes for gasoline production. Isomerization of linear hydrocarbons to branched ones seems to be a good alternative to improve the fuel quality, by increasing the Run Octane Number (RON). Isomerization of alkanes is generally carried out over bifunctional catalysts consisting of an acidic and a metallic function. Sulfated zirconia ($ZrO_2/SO_4$) has attracted intensive attention due to its high catalytic activity for the conversion of small hydrocarbons [1–5]; it is able to catalyze the isomerization of linear to branched light hydrocarbons.

The highly active $ZrO_2/SO_4$ is usually prepared by the sulfatation of amorphous zirconia hydrate followed by a calcination procedure in air. The properties of the resultant $ZrO_2/SO_4$ system strongly depend on the preparation method, that is, on the starting material, sulfatation method, sulfur content, calcinations procedure, and so forth [6].

The catalytic activity of the sulfated zirconia during the alkane isomerization reaction could be largely promoted by the addition of transition metals. The presence of the metal, in an oxidized state, remain in well dispersed state on the zirconia surface stabilizing it against transformation and sintering, and also provides oxidation sites to the sulfated zirconia which improves the isomerization of $n$-alkanes to branched hydrocarbons [7].

It has been established [8,9] that the activity of sulfated zirconia is increased by the incorporation of nickel because it generates active acid sites as Lewis and Bronsted. The increase in activity has been attributed to the generation of additional Brönsted and Lewis acid sites with higher acid strength than those on unpromoted sulfated zirconia. Several attempts [10] have been made in order to correlate the acidity (Bronsted or Lewis) with the catalytic performance of sulfated zirconia. On unpromoted sulfated zirconia, it has been proposed that its isomerization activity can be correlated with the simultaneous presence of Bronsted and Lewis acid sites.

In other hand, the addition of small amounts of NiO to HUSY catalysts induce alkanes isomerization reaction forward the formation of di-branched alkanes more selectively [11], which means the production of higher octane number products, increasing the gasoline quality.

In this paper we report the catalytic behavior of $NiO/SO_4/ZrO_2$ solids in the $n$-hexane isomerization reaction. The concentration of nickel on the catalysts remained in the interval between 0 and 9.6 wt%. The sulfated zirconia catalysts without or with different nickel content used were able to isomerize $n$-hexane at 673 K under 345 kPa of pressure. Well dispersed nickel oxide seems to be responsible for the formation of di-branched $C_6$ isomers, increasing the selectivity toward 2,3 dimethylbutane as main product of the $n$-hexane isomerization reaction.

---

*To whom correspondence should be addressed.

1011-372X/04/0800–0059/0 © 2004 Plenum Publishing Corporation

## 2. Experimental

### 2.1. Synthesis of materials

The synthesis of NiO/$SO_4^{2-}$/$ZrO_2$ samples used in this work was based in a method reported elsewhere [12]. Briefly, an aqueous solution (28 vol%) of ammonium hydroxide (J.T. Baker) was added dropwise to a solution of $ZrO(NO_3)_2$ (Aldrich, 99%) at room temperature until a pH of 9.5 was reached. A white precipitate of $Zr(OH)_4$ was formed. The precipitated was filtered, washed with deionized water and dried at 373 K overnight. The dry hydroxides samples were powdered and divided in seven portions. Sulfated zirconia (SZ) sample was obtained by sulfating one portion of the dry zirconia hydroxide following the incipient wetness method and using a $H_2SO_4$ solution (J.T. Baker, 96 vol%), then the samples were dried at 373 K overnight and then calcined at 948 K in air flow. The nickel containing samples (NSZ) were produced by adding nickel and sulfate simultaneously. In this case $Ni(NO)_3 \cdot 6H_2O$ (Aldrich, 99%) was dissolved in the $H_2SO_4$ solution. Then, the solution was mixed with the dried zirconia hydroxide. The zirconia samples containing nickel and sulfate were dried at 373 K overnight and thereafter the samples were calcined at 948 K in air flow during 4 h. Sulfur content was maintained constant in all the samples around of 4 wt% of the sulfate, and the nickel content varied from 0 to 9.6 wt%. Finally, all samples were manually extruded to 1/8″ cylindrical particles with peptized (1/32 diluted $HNO_3$). All materials were annealed at 948 K for 1 h in flowing air. Samples were coded as X-NSZ, where X indicates the nickel content in wt%, Z stands for zirconium, S for sulfate, N for nickel.

### 2.2. Characterization techniques

The chemical composition was determined by atomic absorption spectroscopy (AAS) in a Perkin Elmer S-2380 apparatus. The sulfur content was determined by combustion in a LECO SC-44 apparatus. Specific surface area measurements were carried out in a Micromeritics Digisorb 2600 apparatus according to ASTM-D-3663. X-ray diffraction patterns of powdered samples were recorded at room temperature with Cu$K_\alpha$ radiation Siemmens D500 diffractometer having $\theta$–$\theta$ configuration and a graphite secondary-beam monochromator. For determination of acidity FT-IR studies were made using a 170-SX Nicolet spectrometer, the samples were evacuated to 0.1 Pa then maintained under flow (2.14 L/h) of nitrogen saturated with pyridine during 15 min. Thereafter, the samples were outgassed 1 h at room temperature, then, they were heated up to the desired temperature using linear temperature program. The total acidity was measured by $NH_3$ titration in an Altamira AMI 2000 apparatus equipped with a thermal conductivity detector (TCD). 200 mg or sample was pretreated under flowing $N_2$ at 773 K for 4 h. Then, the sample was cooled down to 423 K. Calibrated pulses of $NH_3$ were injected through a 6 port on-line valve until saturation of the sample was reached. The amount of $NH_3$ adsorbed by the sample was calculated from the difference between total $NH_3$ injected and the amount of $NH_3$ calculated from the TCD signals.

### 2.3. Catalytic activity

The catalytic activity of solids was studied in the *n*-hexane isomerization reaction. The reaction was carried out in a stainless-steel fixed bed microreactor (7 mm diameter, 150 mm length) using approximately 0.328 g powdered sample previously treated under hydrogen flow (0.249 $cm^3$/min) at 773 K for 1 h. A flow of 0.4 mL/min of *n*-hexane (Matheson C.P.) was fed into the reactor and the reaction temperature was fixed at 673 K. The reaction was carried out at a pressure 345 kPa. The reaction products were analyzed on-line in a Hewlett-Packard 5890 gas chromatograph equipped with a 3 m × 1/8″ packed column (Porasil C) and a thermal conductivity detector (TCD).

## 3. Results and discussion

The chemical compositions of the samples are reported in table 1. The composition of nickel varied from 0 to 9.6 wt%, sulfate content was maintained around 4 wt%, and the zirconia content decreased with the enhancement of the nickel concentration in SZ samples. The textural properties of the X-NSZ samples after calcination at 948 K are also presented in Table 1.

Table 1
Chemical composition and textural properties of the sulfated zirconia promoted with nickel oxide

| Sample | NiO (wt%) | $SO_4^{2}$ (wt%) | $ZrO_2$ (wt%) | Surface area ($m^2\ g^{-1}$) | Pore volume ($cm^3\ g^{-1}$) | Pore diameter (Å) |
|---|---|---|---|---|---|---|
| SZ | 0 | 4.0 | 96 | 66 | 0.108 | 65 |
| 1NSZ | 1.0 | 3.9 | 95 | 62 | 0.108 | 70 |
| 1.5NSZ | 1.5 | 3.9 | 94.4 | 60 | 0.078 | 52 |
| 2.5NSZ | 2.5 | 3.9 | 93.5 | 56 | 0.083 | 39 |
| 4NSZ | 4.5 | 3.9 | 91.5 | 50 | 0.078 | 63 |
| 6NSZ | 6.0 | 3.9 | 90.0 | 66 | 0.072 | 44 |
| 9.6NSZ | 9.6 | 4.0 | 86.4 | 4 | 0.020 | 201 |

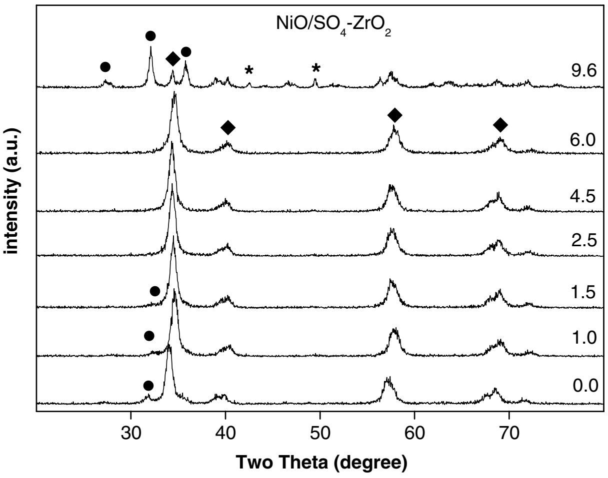

Figure 1. X-ray diffraction patterns of SZ and X-NSZ catalysts annealed at 948 K. (◆)Tetragonal zirconia phase, (●) monoclinic zirconia phase, (*) NiO phase.

The surface areas and the mean porous size varied in the range of 50 to 66 m$^2$/g and from 40 to 70 Å respectively, for the NSZ samples with nickel content between 0 and 6 wt%. However, the variations observed to be not correlated with the increase nickel concentration on the SZ samples. At highest nickel concentration, 9.6 wt%, the NSZ sample showed a very low surface area (4 m$^2$/g) with a big porous size dimension of 201 Å. These changes in porosity are attributed to the phase transformation and sintering processes, such as were observed by X-ray diffraction patterns presented in figure 1. In SZ sample, without nickel, tetragonal and monoclinic zirconia phases coexist in the sample. The monoclinic phase became to disappear at increasing nickel content between 1 and 1.5 wt%, and only tetragonal phase was observed at nickel content between 2.5 and 6 wt%. Thereafter, at increasing nickel content up to 9.6 wt%, practically all the tetragonal phase was transformed into monoclinic phase, and also the diffraction peaks corresponding to the NiO phase appears, suggesting the sintering and growing of promoter nickel oxide on the surface of the zirconia. Then, one can conclude that nickel addition to the sulfated zirconia contribute to stabilize the tetragonal phase remaining in well dispersed state on the zirconia surface at concentration below 6 wt%. At highest nickel content (9.6 wt%), the growing of the NiO phase occurs with larger crystallite size, which causes the transformation of the metastable tetragonal phase into monoclinic phase, with the consequent decrease in surface area and textural properties.

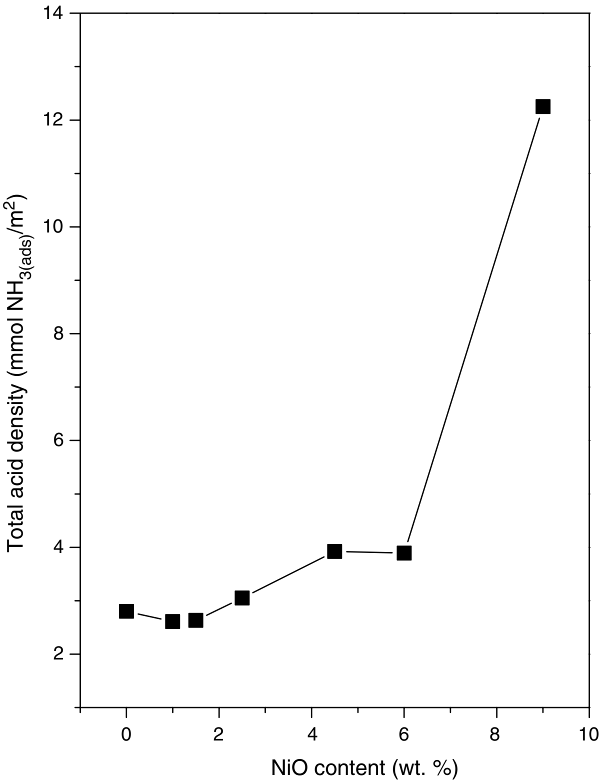

Figure 2. Total acid density measured by $NH_3$ adsorption by TPD analysis versus nickel oxide content.

The acid site density in terms of the specific surface obtained from the $NH_3$ adsorption data is shown in the figure 2. It can be clearly observed that the acid site density showed by the sulfate zirconia is slightly modified by the incorporation of nickel at concentration below to 6 wt%. The total acid site density increased from 2.8 to 3.9 mmol $NH_3$/m$^2$ for the SZ and 6.0NSZ samples respectively. Whereas, at highest nickel content (9.6 wt%) the total acid site density increased to 12.3 mmol $NH_3$/m$^2$, suggesting that higher concentration of acid sites were generated with the segregation of NiO phase and with the transformation of tetragonal into monoclinic zirconia phases. In previous work [13], we reported that nickel addition to the sulfated zirconia did not modify the acid site density, however, the concentration of nickel oxide remained below to 6 wt%. Therefore, it seems that nickel and sulfate groups are both required to stabilize the tetragonal phase and to promote the acid properties of the zirconia.

FT-IR of pyridine adsorption showed the presence of Brönsted and Lewis acid sites in all the samples even outgasing at 573 K. The Brönsted and Lewis acid sites ratio versus nickel content are plotted in figure 3. After evacuation at 323 K, the Brönsted and Lewis ratio decreased as the nickel content increased as consequence of an increase of the Lewis acid site. These results suggest that increase in total acid sites measured by $NH_3$ adsorption with the increase in nickel content, are constituted basically of Lewis acid sites. When the samples were evacuated at 573 K, an increase in the Brönsted/Lewis acid sites ration was observed at nickel concentration between 1 to 4.5 wt.%, thereafter, this acid sites ratio drops to zero value, then, not Brönsted and Lewis acid sites were presented in the samples,

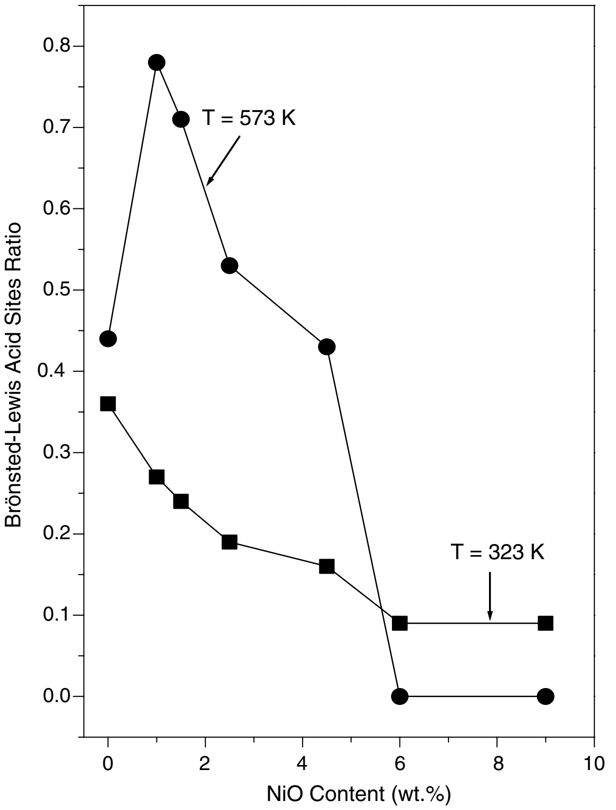

Figure 3. Bronsted–Lewis ratio measured from FT-IR of pyridine adsorption versus nickel oxide content. (■) After evacuation at 323 K and (●) after evacuation at 573 K.

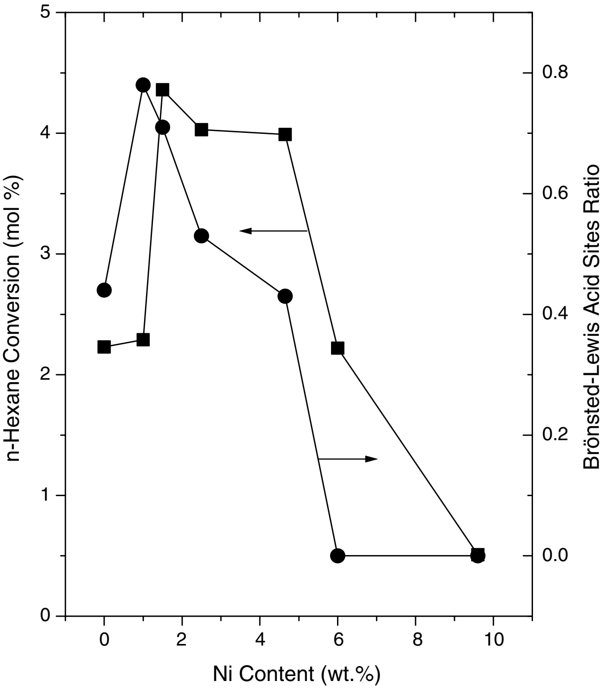

Figure 4. Catalytic and acidic properties versus nickel oxide content. (●) Brönsted–Lewis acid sites ratio. (■) $n$-hexane conversion.

which means that higher concentration of nickel up to 6 wt%, turn off the acidity of the sulfated zirconia. However at nickel concentration between 1 and 4.5 wt%, it seems that nickel contributes to increase the strength of the Brönsted acid sites.

The catalytic activity in $n$-hexane isomerization reaction were developed at conditions in order to obtain low $n$-hexane conversion level ($<5$ mol%) for all the samples, then, deactivation was practically not observed during the 3 h of time on stream evaluated. The $n$-hexane conversion level reached during 1 h of time on stream versus nickel content showed a like-volcano behavior as it is observed in the figure 4. First, The unpromoted sulfated zirconia, SZ sample, and the promoted NSZ sample with 1 wt% of nickel showed a $n$-hexane conversion of 2.2 mol% while the NSZ samples promoted at nickel content between 1.5 and 4.5 showed an increase in $n$-hexane conversion around 4 mol%, then, at increasing the amount on the promoter at 6 wt% the conversion drops to 2.2 mol% again and practically the NSZ sample was inactive to $n$-hexane conversion when the amount of nickel was increased up to 9.6 wt%. Then, it seems that there is an optimum concentration between 1.5 and 4.5 wt% where the nickel could act as a promoter of the activity during $n$-hexane isomerization reaction.

The specific and intrinsic $n$-hexane isomerization activity versus the nickel content on sulfated zirconia samples are plotted in figure 5. Both specific and intrinsic rate showed the like-volcano behavior already observed for the $n$-hexane conversion. Again, there is an optimum concentration of nickel between 1.5 and 4.5 wt%, that contribute to increase the $n$-hexane isomerization activity. Therefore, the contribution of the specific surface area to the catalytic activity could be not relevant, in fact, when intrinsic activity is ploted in figure 5, the like-volcano behavior observed was more pronounced, as consequence of the low specific surface area showed by the samples with 1.5–4.5 wt% of nickel, compared with the other samples, except for the sample with 9.6 wt% of nickel, where sintering, segregation and transformation phases have been occurred.

An attempt to correlate the behavior showed by catalytic activity of the SZ and NSZ samples with their acidic properties are presented also in figure 4. It can be observed that the Brönsted and Lewis acid sites ratio, after out-gassed at 573 K, also increased with the nickel addition. However, the maximum observed was at nickel concentration of 1 wt%, which had low catalytic activity. In fact, the samples with nickel content of 0, 1 and 6 wt% showed the same $n$-hexane conversion level (2.2 mol%) and present quite different B/L ratio 0.44, 0.78 and 0 respectively. Therefore, the catalytic activity can not be attributed only to the increase of the Brönsted acid sites or to the acid sites properties. Nevertheless, several authors have proposed that the driving force in the generation catalysts with very strong

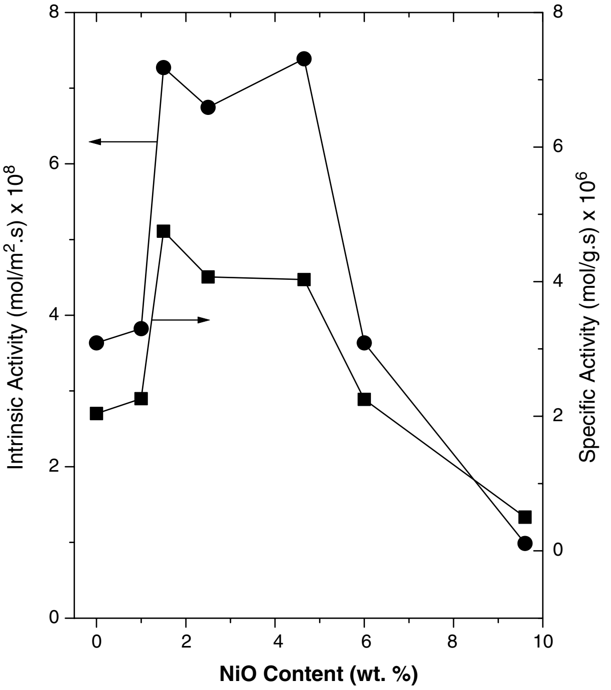

Figure 5. Specific and intrinsic activity during *n*-hexane isomerization reaction versus nickel oxide content on sulfated zirconia.

acidity are the ability of the sulfate to accommodate electrons from a basic molecule increasing in the number and strength of Lewis acid sites. The adsorption of water on these sites implies the formation of Brönsted acid sites [14]. The presence of those Brönsted acid sites allow to carried out *n*-alkanes isomerization reactions at lower temperatures. However, our reactions were made at temperature around 673 K, only Lewis acid sites remain in the samples.

It has been established that the incorporation of the nickel with redox properties to the sulfated zirconia did not show changes in its acidic properties, however, it greatly increases the catalytic activity during *n*-alkanes isomerization reactions [15–17]. From our results we can conclude that nickel incorporation to the sulfated zirconia contributes to increase the strength of the Brönsted acid sites. In addition, nickel incorporation at concentration of 1.5–6 wt% also stabilizes the zirconia tetragonal phase, probably nickel incorporate into the zirconia lattice, forming solid solution, or it remain in strong interaction at the surface of the tetragonal phase inhibiting its transformation into the monoclinic phase. At nickel concentration up to 9.6 wt%, agglomeration and segregation of nickel oxide occurs, the tetragonal zirconia transforms into monoclinic and catalytic activity decreases. Then, the interaction between nickel oxide and zirconia phase is another parameter to take into account in order to explain the catalytic behavior. The strong interaction between nickel and tetragonal zirconia phase lets to have nickel oxide in a well dispersed state, which increase the concentration of oxidic sites with redox properties. These oxidic sites are responsible of the olefins production by a dehydrogenation step, then, the olefins react further with carbocations adsorbed on the acid sites. Therefore, our results support the hypothesis that the *n*-hexane isomerization over $NiO/SO_4/ZrO_2$ take place via bifunctional mechanism [18], involving both acid and oxidic sites. In fact, the dehydrogenation capacity of $ZrO_2–SO_4^{2-}$ has been explained by the acid–base properties of $ZrO_2$ [19–21]. This dehydrogenation capacity greatly enhance by the addition of sulfate and nickel promoters.

The selectivity to the $C_6$ isomers products obtained from the *n*-hexane isomerization reaction is displayed in figure 6. The other products obtained during the reaction were cracking products composed by hydrocarbons from $C_1$ to $C_5$, the selectivity of this product varied from 65 to 70 mol%, as consequence of the high reaction temperature. The SZ and 1NSZ samples produce only monobranched alkanes, such as 2-methylpentane (2MP) and 3-methylpentane (3MP), the *n*-hexane conversion was similar in both catalysts. Increasing nickel content in the samples at concentrations between 1.5 and 4 wt% changes the selectivity toward the production of dibranched alkanes and 2,3-dimethylbutane was obtained with higher selectivity than the monobranched ones. Then, the incorporation of NiO to the sulfated zirconia, not only provide oxidic sites for the initial dehydrogenation step, it orient the reaction toward the production of dibranched alkanes, 2,3-dimethylbutane with RON =

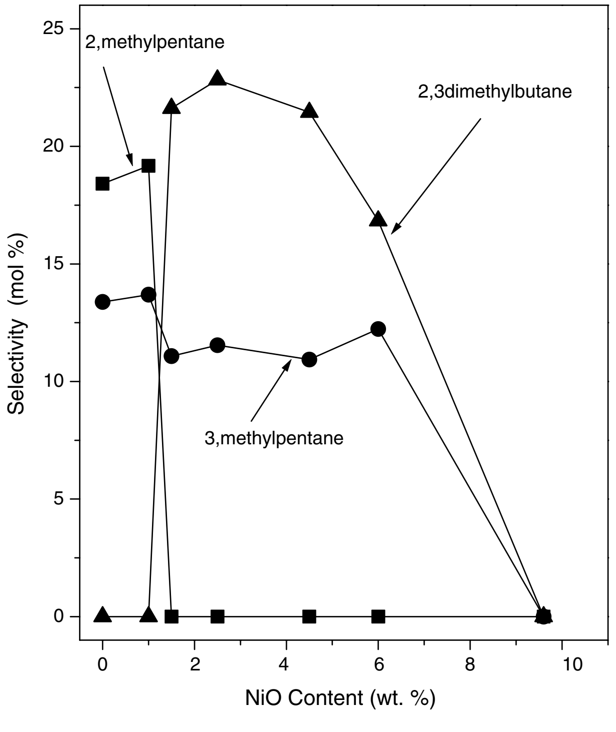

Figure 6. Selectivity toward $C_6$ isomers during *n*-hexane isomerization reaction. (■) 2-methylpentane., (●) 3-methyl pentane., (▲) 2,3-dimethylbutane.

102, a highly desired isomer with higher aggregated value.

## 4. Conclusions

The addition of nickel to the sulfated zirconia contributed to stabilize the zirconia tetragonal phase by establishing a strong interaction between nickel oxide and zirconia, producing a well dispersed nickel oxide on the surface of sulfated zirconia, at nickel oxide concentration between 1.5 and 6 wt%. At this nickel oxide concentration the isomerization reaction properties were promoted increasing the conversion and selectivity toward the dibranched isomer, 2,3-dimethylbutane, a product with higher octane number.

Nickel oxide addition to the sulfated zirconia increased the strength of the Brönsted acid sites. However, the catalytic activity did not correlate only with the acidic properties, suggesting that both acidic and oxidic sites are required, supporting the hypothesis of the bifunctional mechanism.

## References

[1] K. Tanabe, Appl. Catal. 113 (1994) 147.

[2] W. Waqif, J. Bachelier, O. Saur and J.C. Lavalley, J. Mol. Catal. 72 (1992) 127.

[3] M. Bensitel, O. Saur, J.C. Lavalley and B.A. Morrow, Mater. Chem. Phys. 19 (1998) 147.

[4] F. Babou, B. Bigot and P. Sauter, J. Phys. Chem. 97 (1993) 11501.

[5] A. Commeyras and G.A. Olah, J. Am. Chem. Soc. 90 (1968) 2929.

[6] H.H. Davis, R.A. Keog and R. Srinivasan, Catal. Today 20 (1994) 240.

[7] T. Yamaguchi, Appl. Catal. 61 (1990) 1.

[8] J. M. Parera, Catal. Today 151 (1992) 481.

[9] S.C. Fungand and C.A. Querin, J. Catal. 138 (1992) 240.

[10] C.M. Bartholomew and D.G. Mustard, J. Catal. 67 (1981) 186.

[11] W.M.H. Sachtler and Z. Zhang, Adv. Catal. 39 (1993) 129.

[12] M. Perez-Luna, J.A. Toledo, F. Hernandez-Beltran, H. Armendariz and A. Garcia-Borquez, Catal. Lett. 83 (2002) 201.

[13] M. Perez-Luna, H. Armendariz, J.A. Toledo, A. Vazquez, J. Navarrete, A. Montoya and A. Garcia Borquez, J. Mol. Catal. 149 (1999) 169.

[14] A. Corma, V. Fornes, M.I. Juan-Rajadell and J.M. Lopez-Nieto, Appl. Catal. A 16 (1994) 151.

[15] C. Hsu, C.R. Heimbuch, C.T. Armes and B. Gates, J. Chem. Soc., Chem. Commun. (1992) 1645.

[16] V. Adeeva, J.W. de Haan, J. Jänchen, G.D. Lei, V. Shünemann, L.J.M. van de Ven, W.M.H. Sachtler and R.A. Van Santen, J. Catal. 151 (1995) 364.

[17] V. Adeeva, G.D. Lei and W.E. Sachtler, Appl. Catal. 118 (1994) LII.

[18] M. Hino and K. Arata, Catal. Lett. 30 (1995) 25.

[19] D.E. Resaco, H. Liu and W.E. Alvarez, Actas XV Simposio Iberoamericano de Catálisis, Vol. 1, Cordoba, Argentina, 1996, p.191.

[20] D.M. Brouwer and J.M. Oelderik, Rec. Trav. Chim. 87 (1986) 1435.

[21] K. Arata and M. Hino, Mater. Chem. Phys. 26 (1990) 213.